# Isolation and characterization of human thymic epithelial cells

Yong Lin, Madison E Lapine, Deena M Netz, Sarah R Chapin, Rishvanth K. Prabakar, Hannah V Meyer

Downloaded from academic.oup.com/jimmunol/article/215/11/vkag281/9045887 by Cold Spring Harbor Laboratory user on 16 November 2026



*The Journal of Immunology*, 2026, 215(11), vkag281
https://doi.org/10.1093/jimmun/vkag281
**Research Article**

American Association of Immunologists™ OXFORD

# Isolation and characterization of human thymic epithelial cells

**Yong Lin, Madison E. Lapine, Deena M. Netz, Sarah R. Chapin, Rishvanth K. Prabakar, Hannah V. Meyer*,**

Simons Center for Quantitative Biology, Cold Spring Harbor Laboratory, Cold Spring Harbor, NY, United States
*Corresponding author: Email: hmeyer@cshl.edu

## Abstract

**The human thymus is critical for establishing a functional adaptive immune system, with reduced cancer risk, increased healthy aging, and longevity all linked to its function. However, the molecular and physiological mechanisms of these associations are incompletely understood. For the reproducible identification of mechanisms and mitigating cell types, consistent tissue processing and analysis techniques are essential. Here, we assessed biological and technical parameters for the processing, isolation, and analyses of human thymic epithelial cells (TECs). We found that EpCAM and autofluorescence emissions in the range of 500 to 650 nm excited by the 405 nm laser are sufficient to distinguish TECs from other thymic cells, particularly the autofluorescent population. We identified CD205 as the target of the classical cortical TEC antibody CDR2 and re-established CD205 as a reliable marker to distinguish cortical and medullary TECs, which we confirmed by single-cell RNA sequencing. In a systematic comparison of sample processing and digestion conditions, we assessed representative tissue sample size and protein staining patterns, which enabled us to clarify and reconcile inconsistencies across previously published results. Lastly, we established a minimal flow cytometry panel sequencing for the isolation of major TEC populations and their developmental stages. In summary, we provide recommendations to improve reproducibility in the study of human TEC biology and thymus function.**

**Keywords** cell isolation, cell type annotation, flow cytometry parameters, gating strategy, thymic epithelium

## Introduction

The human thymus is critical for the development of a functional yet self-tolerant T cell population. Thymic epithelial cells (TECs) are a rare cell type within the thymus, representing <1% of all thymic cells after birth.[1,2] They can be classified into two major subsets based on both tissue location and function. CD205+ cortical TECs (cTECs) are located in the thymic cortex and provide survival signals to thymocytes with functional T cell receptors. CD205− medullary TECs (mTECs) make up the medulla of the thymus and are critical for eliminating self-reactive thymocytes or redirecting them into regulatory T cell lineages. The importance of TECs is best demonstrated by disorders caused by their developmental defects. For example, mutations in FOXN1, a transcription factor essential for TEC development, result in severe immunodeficiency associated with little or no T cells.[3,4] Similarly, mutations in AIRE, a transcriptional regulator expressed in mTECs, result in widespread autoimmune symptoms.[5] Much work has been done in the past forty years to better understand TEC biology with the aim of therapeutic advances that can repair thymic defects in infants or rejuvenate the thymus in old age.

Single-cell sequencing techniques have enabled high-resolution characterization and lineage tracing of TECs, shedding light on the variety of TEC subtypes and their developmental relationships in humans and model organisms.[6–11] These higher resolution methods have elevated the importance of the initial tissue processing step, as minor differences in processing conditions may influence the sensitive transcriptomic state of the cells, leading to irreproducibility of results such as cell type annotation and progenitor-progeny relationships. Similarly, biases in cell isolation may promote the selection of one cell subset and the depletion of another.[12] In this scenario, even if the transcript quality is excellent, missing cell subsets can negatively affect analytical techniques such as lineage tracing, which necessitate that no missing links exist in the dataset.

A consistent and reproducible thymus tissue processing workflow is essential to accelerate our understanding of TEC biology as well as therapeutic development for thymus repair. TEC studies are particularly challenging due to low TEC frequency and strong adherence to tissue matrix, requiring extensive enzymatic digestion and enrichment steps. Human thymus samples add an additional layer of complexity due to large organ size and therefore sampling variance caused by tissue size and location. To

**Received:** May 20, 2026. **Revised:** August 28, 2026. **Accepted:** September 23, 2026
© The Author(s) 2026. Published by Oxford University Press on behalf of The American Association of Immunologists.
This is an Open Access article distributed under the terms of the Creative Commons Attribution-NonCommercial License (https://creativecommons.org/licenses/by-nc/4.0/), which permits non-commercial re-use, distribution, and reproduction in any medium, provided the original work is properly cited. For commercial re-use, please contact reprints@oup.com for reprints and translation rights for reprints. All other permissions can be obtained through our RightsLink service via the Permissions link on the article page on our site—for further information please contact journals.permissions@oup.com.

Downloaded from academic.oup.com/jimmunol/article/215/11/vkag281/9045887 by Cold Spring Harbor Laboratory user on 16 November 2026

promote consistency across human TEC studies and minimize potential biases, we investigated key parameters of the tissue processing workflow, including tissue size, digestion conditions, and light-scatter characteristics of TECs by flow cytometry. Recent studies have identified additional markers for classical TEC subsets as well as novel subsets, including putative thymic epithelial stem cells (TESCs)[11,13] and CD24+ mTECs, which mirror the phenotypes of peripheral cell types.[11] Variations in expression of these markers across studies led us to characterize the expression of these markers across different tissue processing conditions. Based on these experiments, we developed a minimal flow cytometry panel and gating strategy for the consistent identification of major TEC subsets using surface markers that show concordance in both RNA and protein expression.

# Methods

## Human thymic epithelial cell enrichment

### Tissue samples

Discarded thymus tissues obtained from human donors undergoing medically necessary surgery were collected under the Mount Sinai Biorepository with a Waiver of Consent. Additional tissue was collected under the Northwell Health Biospecimen Repository (Institutional Review Board 20-0150) with patient consent. The use of these human tissues was reviewed by the Cold Spring Harbor Institutional Review Board. Data in this study were generated from 15 human thymus samples (6 females and 9 males). The ages ranged from 4 days old to 4 years old, with a median and mean age of 90 days and 241 days. Additional information, including reason for surgery and the data source for each figure, can be found in the Table S1.

### Thymocyte release

Human thymus samples were processed as soon as possible following their extraction during surgery. A total of 1.2 to 2.0 g of tissue were taken to be processed for analysis (Fig. S1). The tissue was placed in Tissue Buffer containing RPMI 1640 without phenol red (Gibco 11835055), 5% heat-inactivated fetal bovine serum (FBS) (Corning 35-010-CV), 1× penicillin/streptomycin (Gibco 15070063), and 10 mM HEPES (Gibco 15630080) in a 6-well tissue culture dish and further dissected into smaller pieces. As estrogen was reported to mediate the downregulation of AIRE expression, we avoided the use of phenol red due to its potential as an estrogen mimic.[14] The pieces were then transferred to a 50 mL falcon tube for thymocyte release. A total of 25 mL of ice-cold Tissue Buffer was added to the tissue pieces and the tube repeatedly inverted for 1 min to release the thymocytes, followed by 1 min rest on ice. These two steps were repeated for a total of 3 times before the supernatant containing the thymocytes were collected. In total, 4 rounds of thymocyte release were performed.

### Tissue digestion

The tissue pieces underwent 3 rounds of digestion with 9 mL of a digestion solution containing RPMI 1640 without phenol red, 2% heat-inactivated FBS, 20 mM HEPES, 80 U/mL DNase I (MilliporeSigma 11284932001), 0.8 U/mL Dispase I (Worthington LS02104), and 0.6 mg/mL Collagenase IV (Worthington LS004188) for 25 min at 37 °C. After each round, the supernatant containing the released cells was transferred to 20 mL of ice-cold Tissue Buffer containing 1 mM EDTA to stop the digestion process. Typically, 2 to 3 rounds of digestion are sufficient. Following the initial digestion step, an additional digestion step using TrypLE Express without phenol red (Gibco 12604013) supplemented with 100 U/mL DNase I, 1 mM $MgCl_2$, and 2 mM $CaCl_2$ was performed at 7 mL/1g of starting tissue for 5 min at 37 °C. Ice-cold Tissue Buffer (5 times the volume of TrypLE Express used) was added to stop the digest and the cells were filtered through a 100 μm nylon cell strainer to remove residual tissue. Cells were spun down at 350 *g* for 10 min at 4 °C to remove the TrypLE Express solution and washed once with 9 mL of Enrichment Buffer containing 1× Hanks' Buffered Salt Solution (HBSS) (Gibco 14175103), 4% heat-inactivated FBS, 60 U/mL DNase I, and 10 mM of HEPES.

### Enrichment by panning

The enrichment of TECs was by negative selection using the panning method.[15–17] To prepare panning plates, 50 μg of goat anti-mouse IgG (Jackson ImmunoResearch 115-005-062) in 4 mL of Tris pH 9.5 was added per 100 × 15 mm petri dish (VWR 25384-242) and incubated at room temperature for at least 1 h to allow the antibodies to bind to the plates. The antibody solution was then removed and the plates washed 3 times with 1× phosphate-buffered saline (PBS) and then stored with 1× PBS at room temperature until ready to use. Following the tissue digestion step with TrypLE, cells were stained with a mouse anti-human antibody cocktail (anti-human CD3 clone UCHT1, anti-human CD4 clone RPA-T4, anti-human CD8 clone RPA-T8, anti-human CD45 clone HI30, and anti-human CD235a clone HI264, all purchased from BioLegend) for 30 min on ice. Cells were washed twice with Enrichment Buffer before resuspending in the same buffer. A total of 1 to $1.5 \times 10^9$ cells were split equally into 5 panning plates and incubated at room temperature to allow the thymocytes to adhere to the plates. The nonadherent cells were collected and transferred equally to another set of 5 panning plates. A minimum of 3 rounds of panning were performed. The nonadherent cells containing the enriched TECs were harvested for downstream assays such as flow cytometry and cell sorting.

For the experiment comparing different digestive enzyme cocktails on cell marker expression by flow cytometry, 1.2 g of tissue were collected at 4 locations of the thymus. These tissue chunks were diced into smaller pieces, pooled, and mixed well to minimize differences across tissue locations. After the thymocyte release step, the pooled tissue pieces were divided into 4 portions, each subjected to a different digestion enzyme cocktail. Subsequent TEC enrichment by panning was as described previously.

## Flow cytometry and FACS of human TECs and thymocytes

Enriched TECs were spun down at 350 *g* for 5 min at 4 °C. Cells were treated with Fc Block (BioLegend 422302) for 10 min on ice prior to staining with the fluorophore-conjugated antibody

Downloaded from academic.oup.com/jimmunol/article/215/11/vkag281/9045887 by Cold Spring Harbor Laboratory user on 16 November 2026

cocktail for 30 min on ice. The list of anti-human antibodies used is as follows (Target-Fluorophore Clone): EpCAM-BV421 clone 9C4, EpCAM-BV421 clone CO17-1A, CD45-FITC clone HI30, CD45-AF647 clone HI30, CD205-PE clone HD30, CD205-AF647 clone HD30, cTEC antibody CDR2-AF647 and CDR2-AF488 (both generously gifted by Dr. Sheena Pinto), CD200-BV605 clone OX-104, CD200-AF647 clone OX-104, CD49f-PE/Cy7 clone GoH3, BCAM-PE clone QA20A43, BCAM-BV605 clone B64 (BD Biosciences 748008), CD104-PE clone 58XB4, CD24-AF488 clone ML5, and Pdpn-PE clone NC-08. Unless otherwise noted, all antibodies were purchased from BioLegend. All stainings were carried out in 1× HBSS due to the use of fixable viability dye, Fixable Near-IR (Invitrogen L10119), that is incompatible with buffers containing proteins such as FACS buffer. After staining, cells were washed twice with FACS buffer (1× PBS without calcium or magnesium, 3% FBS, 0.05% w/v sodium azide) to quench the residual fixable viability dye and then fixed with 2% PFA for 30 min on ice. After fixation, cells were washed twice with 1× PBS and then resuspended in FACS buffer. Fixed cells were stored on ice in 4 °C until ready to be analyzed by flow cytometry. The flow cytometer used in this study is the BD LSRFortessa Cell Analyzer. The cell sorter used in this study is the Sony SH800 cell sorter.

In the experiment to assess CD200 expression in thymocytes, $2 \times 10^6$ thymocytes from the thymocyte release step were taken for staining. The following antibodies were used: CD4-FITC clone A161A1 (BioLegend 357405), CD8α-BV421 clone RPA-T8 (BioLegend 301035), CD200-AF647 clone OX-104 (BioLegend 329214), and Fixable Near-IR. The cells were first treated for 10 min with Fc Block to minimize nonspecific binding and then stained with the antibodies in 1× HBSS buffer for 30 min on ice. After staining, cells were washed twice with FACS buffer and fixed with 2% PFA for 30 min on ice. After fixation, cells were washed twice in 1× PBS and then resuspended in FACS buffer before analyzing on the flow cytometer.

## Detection of CDR2 antibody target using THP-1 human monocyte cell line

THP-1 cells were grown in RPMI 1640 culture media supplemented with 10% FBS and 1× penicillin/streptomycin. A total of $1 \times 10^6$ cells were taken for each blocking condition. Blocking antibodies were purchased from the following vendors: R&D Systems (polyclonal, immunogen: *Escherichia coli*–derived recombinant human DEC-205/CD205 Cys216-Cys501, cat# AF2047-SP), LSBio (polyclonal, immunogen: recombinant human lymphocyte antigen 75 protein [440-680AA], cat# LS-C676008-50), BioLegend (monoclonal, clone HD30, cat# 342202). During the blocking step, human Fc Block (BioLegend; cat# 422301) and Monocyte Blocker (BioLegend; cat# 426101) were also added to minimize nonspecific interactions. After blocking for 20 min on ice, cells were stained with the same amount (1 μg) of CDR2 antibody (conjugated to AF647) for 30 min on ice. After staining, cells were washed with FACS buffer and fixed in 2% PFA for 30 min on ice. After fixation, cells were washed with 1× PBS and resuspended in FACS buffer until ready to be analyzed by flow cytometry.

## Assessing CDR2 recognition of purified LY75 protein by dot blot

Purified LY75 (CD205) protein (LY75-his-tagged) was purchased from acro biosystems (cat# LY5-H52H3). The lyophilized protein was reconstituted in 250 μL of sterile deionized water to a concentration of 400 μg/mL and stored at −80 °C. For the dot blot, 0.8 μg of stock LY75 was added to the center of 3 nitrocellulose membrane squares and let dry for at least 10 min. The membrane was then blocked with 5% bovine serum albumin (BSA) in PBST (1× PBS containing 0.05% v/v Tween 20) for 2 h at 4 °C. After blocking, membranes were stained with either 0.5 μg/mL of CDR2 antibody, 0.5 μg/mL CD205 antibody (clone HD30, positive control), or 0.5 μg/mL CD3 antibody (clone UCHT1, negative control), for 3 h at 4 °C. After staining, membranes were washed 3 times with PBST on a horizontal shaker for 5 min per wash. After washing, membranes were incubated with donkey anti-mouse-horseradish peroxidase secondary antibody at a final concentration of 0.16 μg/mL for 30 min at room temperature. Membranes were again washed in PBST 3 times for 5 min each before incubating in the TMB-M substrate solution (Rockland Immunochemicals TMBM-100) for 45 min at room temperature to detect antibody binding to the LY75 protein.

## 10x Genomics Flex single-cell RNA sequencing analysis

Three human thymus samples (sample ID: HT67, HT70, HT71) were used for the 10x Genomics Flex single-cell RNA sequencing (scRNAseq) experiment. TEC processing and enrichment steps were as described previously. After enrichment and staining for FACS, cells were fixed following the 10x Genomics Flex scRNAseq sample preparation protocol from 10x Genomics. A total of 1 mL of the 10x Genomics Flex fixation buffer (nuclease-free water, concentrated Fix & Perm Buffer, and formaldehyde 37% stock) was used per $10 \times 10^6$ cells. The samples were fixed at 4 °C for 10 or 16 h (as specified in Table S1). After fixation, cells were spun down at 850 *g* for 5 min at room temperature and resuspended in Tissue Resuspension Buffer (0.496× PBS, 50 mM Tris Buffer, 0.02% RNase-free BSA, 0.24 U/μL Protector RNase Inhibitor). Cells were sorted for all EpCAM+ cells (sample ID HT70 and HT71), EpCAM+ CD205− cells (sample ID HT67), or EpCAM + CD205+ cells (sample ID HT67). The sort collection buffer was 500 μL of 1% Nuclease-free BSA solution in 0.5× PBS, containing 0.4 U/μL of Protector RNase Inhibitor. After sorting, cells were spun down at 850 *g* for 5 min at room temperature and resuspended in 500 μL 10x Genomics Flex Quenching buffer containing 0.2 U/mL of Protector RNase Inhibitor. A total of 50 μL of prewarmed enhancer solution and 137.5 μL of 50% glycerol solution were added sequentially and the samples frozen down in a Mr. Frosty container in −80 °C freezer. Frozen samples were submitted to the Single Cell Sequencing Facility and sequenced in the same run. Raw read counts were generated using Cell Ranger v9.0.1 (10x Genomics) and aligned to GRCh38-2020-A human reference using probe set v1.0.1. Data were processed and cell types annotated using Seurat version 5.5.1.[18] For the quality control filtering steps for each sample, the mitochondrial gene percentage cutoff was set at 3 standard deviations above the mean. The feature counts cutoff was set between 500 features

Downloaded from academic.oup.com/jimmunol/article/215/11/vkag281/9045887 by Cold Spring Harbor Laboratory user on 16 November 2026

(lower threshold) and 3 standard deviations above the mean (upper threshold). Default values were used for the standard analysis steps *NormalizeData*, *FindVariableFeatures*, *ScaleData*, and *RunPCA*. Annotation of the cell clusters were based on expression of the following lineage markers: cTEC (TBATA, PRSS16, PSMB11, LY75), mTEC lo (CLU, CCL19, KRT15, KRT19, FN1), mTEC hi (AIRE, FEZF2), Nurse (TBATA, PRSS16, PSMB11, CD3E, PTPRC), Mimetic TEC (CD24), basement membrane collagen (BMC)–enriched TEC (BMC TEC) (COL4A5, COL4A6, COL8A1), Endothelial (PECAM1), Pericytes (PDGFRB, RGS5), and Erythroid (CA1, HBB, HBA2). In addition to these clusters, we identified cluster 7 which defines a TEC population spanning the entire Uniform Manifold Approximation and Projection (UMAP) space in our data (Fig. S2A) as well as the integration of our data with the thymic stromal cell atlas by Bautista et al.[7] When we assessed the differential gene expression profile of each UMAP subregion of cluster 7, they showed an expression pattern spanning multiple TEC subtypes. Due to the scattered UMAP distribution and gene expression profile, this cluster is most likely an technical artifact, even though it passed the quality control filters. We did not consider this cluster in further downstream analyses.

## 10x Genomics Flex and Bautista integration

The Bautista data were reprocessed from the original FASTQ files downloaded from https://www.ncbi.nlm.nih.gov/geo/query/acc.cgi? acc=GSE147520. *STARsolo* (preprint located at https://www.biorxiv.org/content/10.1101/2021.05.05.442755v1) was used to align the reads to GRCh38 (primary assembly) using Gencode annotation version V44, as well as to generate the count matrix. Cells with a mitochondrial gene percentage >15% and with fewer than 200 expressed genes were removed from downstream analysis, as were cells that did not have prior published annotations. The data was normalized in scanpy[19] via *sc.pp.normalize* with a target_sum = 1e4. Log normalization was performed via *sc.pp.log1p*, and the top 3,000 highly variable genes were selected. The 10x Genomics Flex and Bautista datasets were integrated via *scVI*[20,21] with 3 categorical batch covariates: sequencing protocol, donor, and study. The data were further integrated in a semi-supervised manner via scANVI[22] with high-level cell type labels (TEC, endothelial cell, immune cell, mesenchyme cell, mesothelial cell, nurse cell, pericyte, and red blood cell) as input.

## MuSiC deconvolution analysis

To determine the TEC subset that the CD49f(hi)CD200− population projects onto, we used the R package MuSiC: Multi-subject Single-cell Deconvolution.[23] The published bulk RNA sequencing FASTQ data from Haunerdinger et al. (https://www.ebi.ac.uk/ena/browser/view/PRJEB39649)[13] were downloaded on July 18, 2024, and gene counts were generated using STAR version 2.7.8.[24] MuSiC version 1.0.0 was used for the deconvolution analysis with our 10x Genomics Flex scRNAseq TEC dataset used as the reference.

# Results

## EpCAM and autofluorescence parameters are sufficient to identify human TECs

Isolation approaches for human TECs vary from study to study, but a typical workflow involves 5 major steps: tissue dissection, thymocyte release, enzymatic digestion, enrichment, and flow cytometric analysis or sorting for downstream assays (Fig. S1). The flow cytometry gating strategy for the identification of human TECs is then traditionally based on the expression of EpCAM and the hematopoietic marker CD45, in which TECs are EpCAM + CD45−.[25,26] More recently, Haunerdinger et al.[13] proposed an alternative approach, identifying TECs as EpCAM + Pdpn+. We find that simply analyzing EpCAM against cell-intrinsic autofluorescence signals in an open detector in the 500 to 650 nm wavelength range, excited by low-wavelength lasers (405 nm Violet laser or 488 nm Blue laser), is sufficient to identify the human TEC population by flow cytometry (Fig. 1A, bottom center plot). Visualizing Pdpn expression after gating on TECs using EpCAM vs autofluorescence, we show agreement of this approach with the EpCAM versus Pdpn approach (Fig. 1A, bottom left plot versus bottom right plot). Importantly, this approach bears the advantage of minimizing potential non-TEC autofluorescent cells mixed in with the EpCAM + Pdpn + cells depending on the fluorophore combination used and avoids the use of an additional antibody. Compared with the frequency of cells in the autofluorescence approach, the use of CD45 led to a decrease in cell frequency (Fig. 1B). While TECs do not express CD45, intercellular transfer of proteins between TECs and immune cells has been reported, which may explain the expression of CD45 on some TECs.[27–38]

## CD205 is a reliable marker for the identification of human cTECs

The CDR2 monoclonal antibody was traditionally used to identify human cTECs.[39] This antibody recognized an unknown target and was not available commercially. CD205 (LY75) was later identified as an alternative cTEC marker to identify human cTECs in flow cytometry and scRNAseq analysis[40–42] but its reliability has recently been questioned.[13] To overcome the reliance on CDR2 antibody and confirm the dependability of CD205 as a cTEC marker, we performed a series of experiments using primary human TECs, purified CD205 protein, and a CD205-expressing cell line. Compared with CDR2, CD205 antibody clone HD30 showed a near identical staining pattern on primary TECs albeit at a lower signal intensity (Fig. 2A).[39] Plotting CDR2 and CD205 expressions against each other results in a narrow diagonal staining pattern (Fig. 2A, right), indicating that either these two antibodies target different epitopes on the same antigen or they target two different antigens whose expressions are tightly correlated. To assess whether the epitope of the CDR2 antibody is on CD205, we performed a dot blot experiment using purified human CD205 protein. We showed that the CDR2 antibody indeed stains the purified CD205 protein (Fig. 2B). Similarly, we showed that the human cell line THP-1 that expresses CD205[43] stained positively with the CDR2 antibody (Fig. 2C). To identify the exact region of the epitope, we performed a blocking

Downloaded from academic.oup.com/jimmunol/article/215/11/vkag281/9045887 by Cold Spring Harbor Laboratory user on 16 November 2026

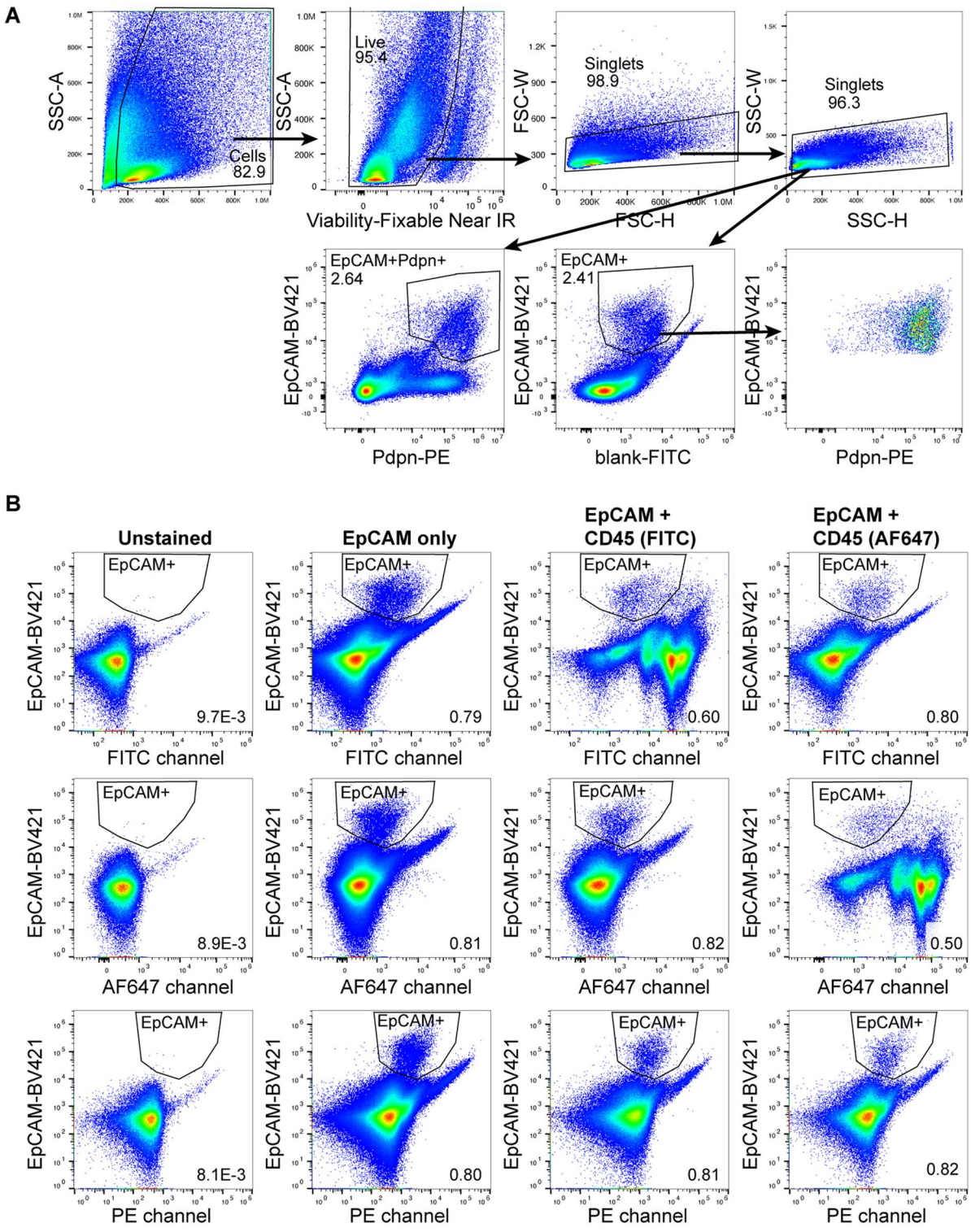



**Figure 1** Identification of human TECs by EpCAM and autofluorescence. (A) Comparison of the EpCAM and autofluorescence approach with the EpCAM and Pdpn approach to identify human TECs,[13] showing that these approaches are equivalent. (B) Comparison of the EpCAM and autofluorescence approach with the EpCAM and CD45 approach to identify human TECs. Results indicate that some EpCAM + cells are positive for CD45. Multiple fluorophore-conjugated CD45 antibodies were used to demonstrate robustness of the results. FSC-H, forward scatter height; FSC-W, forward scatter width; SSC-H, side scatter height; SSC-W, side scatter width.

experiment using two CD205 polyclonal antibodies (LSBio antibody immunogen: CD205 amino acid sequence 440–680; R&D Systems antibody immunogen: CD205 amino acid sequence 216–501). Our data indicated that preincubation with the R&D Systems CD205 polyclonal antibody reduced the staining signal intensity of the CDR2 antibody, suggesting that the CDR2

Downloaded from academic.oup.com/jimmunol/article/215/11/vkag281/9045887 by Cold Spring Harbor Laboratory user on 16 November 2026

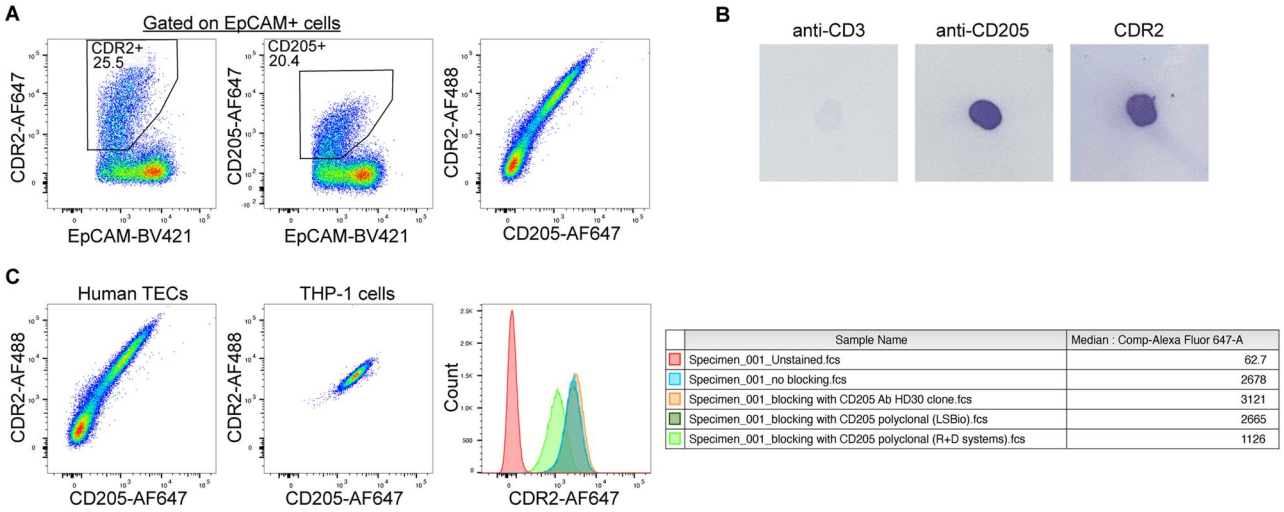



**Figure 2** CD205 is a reliable marker for human cTECs. (A) Human TECs stained with the cTEC antibody CDR2 and the CD205 antibody. The left two plots demonstrate positive staining of CDR2 and CD205 primarily in TECs expressing relatively lower expression of EpCAM. The right plot demonstrates a diagonal staining pattern between CDR2 and CD205, suggesting the same protein target. (B) Dot blot of purified CD205 protein stained with anti-CD3 antibody (negative control), CDR2 antibody, or anti-CD205 antibody (positive control), showing CD205 is targeted by the CDR2 antibody. (C) THP-1 cell line, which expresses CD205, is stained positively by the CDR2 antibody. Staining of THP-1 cells by CDR2 can be partially blocked by the polyclonal anti-CD205 antibody from R&D Systems targeting CD205 protein amino acid positions 216 to 501.

antibody binds somewhere within the CD205 amino acid sequence 216–501 (Fig. 2C, right).

## Assessing a representative tissue sample of a human thymus

A human thymus can weigh more than 30 g. To properly assess the TEC composition of the human thymus yet maintain protocol practicality, we tested whether a given amount of tissue from different locations was representative, using the cTEC: mTEC ratio as a proxy. We found that the proportion of cTECs to mTECs is consistent across 4 different regions of the same thymus for tissue size of about 1 g (in these data, the tissue measured approximately 1.2 g), indicating that this size, while may not be the minimum, is a representative sample of a neonatal (4 mo old) human thymus in terms of TEC composition (Fig. 3). For all subsequent experiments, we used tissue sizes of at least 1.2 g in size (usually 1.5–2.0 g, depending on downstream assay needs).

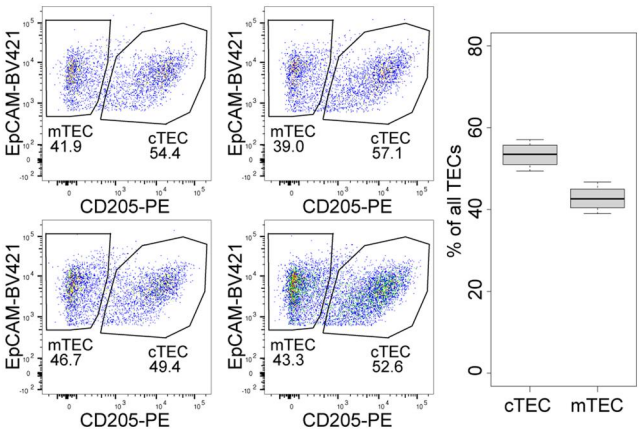



**Figure 3** Assessing a representative tissue sample of a human thymus. Quantification of mTEC (EpCAM+ CD205−) to cTEC (EpCAM+ CD205+) proportions from four 1.2 g tissue pieces taken from 4 distinct locations in a neonatal human thymus, demonstrating that this tissue size contains a representative sample of the thymus in terms of cortex to medulla percentage.

## scRNAseq analysis confirms flow cytometry gating strategy and clarifies TEC subset markers

To confirm TEC subset identities, we sorted out CD205+ TECs, CD205− TECs, or all TECs and performed scRNAseq on each of these subsets. We observed strong expression of cTEC-specific markers (PSMB11, PRSS16, LY75)[44] in the sorted CD205+ TECs, further supporting our gating strategy based on EpCAM, autofluorescence, and CD205 (Fig. 4A, B; Figs. S2 and S3). In total, we identified the 5 major known human TEC subsets based on known marker genes unique to them: cTEC, thymocyte-enclosing nurse cells, immature mTEC lo, AIRE-expressing mTEC hi, and a group of so-called mimetic TECs, mirroring expression of peripheral cell types such as tuft cells, ionocytes, and muscle cells,[8,9] as well as small clusters of endothelial cells, pericytes, and erythroid cells (Figs. S2 and S3), likely due to sorting impurity. Additionally, we identified a transcriptionally distinct subset of cells with limited to no expression of cTEC (CD205) and mTEC (CLU, AIRE, FEZF2) or mimetic cell markers (CD24) (Fig. 4B; Figs. S2 and S3). Due to their enrichment for basement membrane-associated collagen genes including COL4A5 and COL4A6, we named these cells BMC TECs (Fig. 4B; Fig. S3). We also noticed a high expression of the integrin ITGB4 in the BMC TECs relative to other TECs (Fig. 4B; Fig. S3). Importantly, there were no distinct clusters corresponding to thymocytes in the scRNAseq data,

Downloaded from academic.oup.com/jimmunol/article/215/11/vkag281/9045887 by Cold Spring Harbor Laboratory user on 16 November 2026

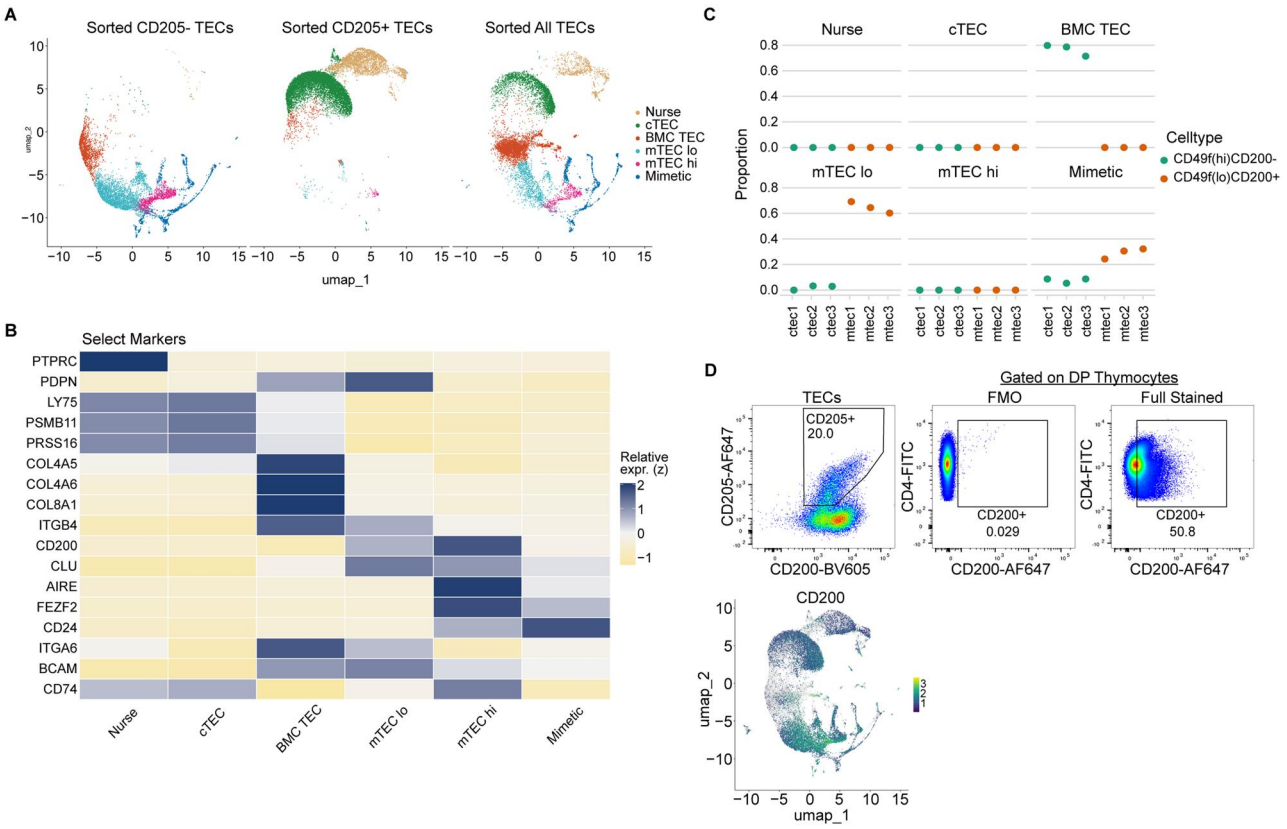



**Figure 4** scRNAseq analysis confirms flow cytometry gating strategy and clarifies TEC subset markers. (A) UMAP of sorted TECs, CD205− TECs, and CD205+ TECs. (B) Expression of select markers for TEC subsets: cTECs are defined by PRSS16, PSMB11, and LY75. Nurse cells are defined by cTEC markers and express immune marker PTPRC derived from its internalized thymocytes. BMC TECs are enriched for basement membrane collagens (COL4A5, COL4A6, COL8A1) and ITGB4 expression. CLU defines mTEC lo, with lower expression in BMC TECs and mTEC hi. mTEC hi uniquely expresses high levels of AIRE and FEZF2. High expression of CD24 defines the majority of mimetic TECs. ITGA6 is expressed at an intermediate level across the TEC subsets. BCAM is expressed across BMC TEC and mTEC subsets. (C) MuSiC deconvolution analysis indicates that CD49f(hi)CD200− TECs mostly map to BMC TECs in our scRNAseq dataset. (D) Expression of CD200 in TECs by flow cytometry and scRNAseq. (Right) Expression of CD200 by double-positive (DP) thymocytes. FMO, fluorescence minus one.

indicating that the CD45-expressing TECs (Fig. 1B) are not doublets of TECs and thymocytes.

The basement membrane collagens COL4A5 and COL4A6 were described as highly expressed in human CD49f(hi)CD200− TECs, a population classified as cTECs.[13] Based on our scRNAseq data, COL4A6 expression is highly restricted to the BMC TECs and not expressed in any other TEC subsets. Also, most of the BMC TECs express little to no CD200 (Fig. 4D, bottom). We suspected that the CD49f(hi)CD200− TECs previously identified as cTECs are actually the BMC TECs. To assess this, we performed deconvolution analysis on the published bulk RNAseq data of the CD49f(hi)CD200− TECs using our scRNAseq data as cell type reference. We found that more than 70% of TECs in the bulk RNAseq data were derived from BMC TECs and not cTECs, indicating that the CD49f(hi)CD200− TECs are mainly composed of a unique TEC population expressing high levels of basement membrane–associated collagen genes (Fig. 4C). To place the BMC TEC population into the context of other canonical TEC subtypes reported to lack expression of genes characteristic of cTECs or mTECs, we integrated our data with the stromal thymus atlas by Bautista et al. (Fig. S4A)[7] and assessed BMC TEC expression of reported marker genes of immature[7] and PolyKRT TECs.[11] After integration, BMC TECs overlapped with cell types classified as early in TEC development (immature TEC, cTEC lo, and mTEC lo) (Fig. S4A) by Bautista et al.[7] By gene signature, BMC TECs matched most closely with the provisionally labeled "immature TECs" reported (Fig. S4B). In contrast, the module score of signature markers of the PolyKRT TECs was highest in the mTEC lo population (74.5% of the 10,000 cells that express the highest PolyKRT module score), followed by BMC TECs (16.4% of the 10,000 cells that express the highest PolyKRT module score) (Fig. S4C, D).

We then assessed CD200 expression against CD205 expression in our flow cytometry data and observed that the CD205+ TECs actually expressed CD200 at least as highly as mTECs (Fig. 4D, left). Surprisingly, mTECs seem to express higher levels of CD200 at the messenger RNA (mRNA) level compared with cTECs based on the scRNAseq data (Fig. 4D, bottom). It is possible that mRNA and protein levels of CD200 show poor correlation in human TEC subsets, similar to its expression in other tissues (Fig. S5). Alternatively, there may be intercellular transfer of CD200 protein from thymocytes to cTECs. cTECs interact closely with double-positive thymocytes in the cortex, even internalizing thymocytes to support positive and negative selection.[45–47] We

Downloaded from academic.oup.com/jimmunol/article/215/11/vkag281/9045887 by Cold Spring Harbor Laboratory user on 16 November 2026

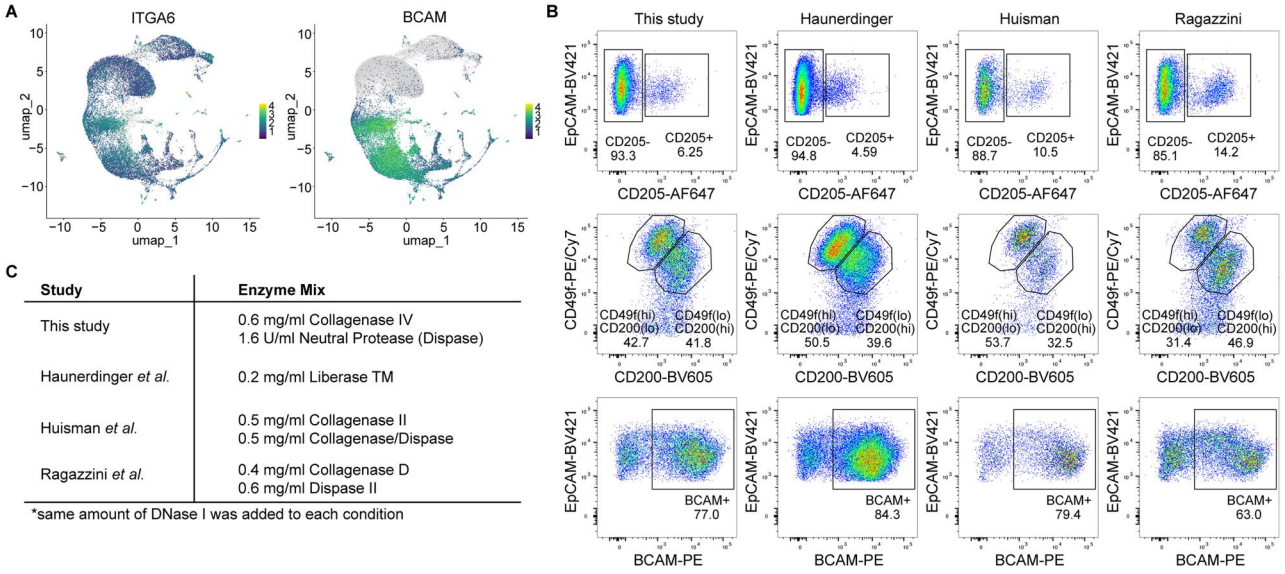
hypothesized that if cTECs inherit CD200 protein from another cell type, then they are most likely double-positive thymocytes. Indeed, by flow cytometric analysis, double-positive thymocytes appear positive for CD200 expression (Fig. 4D, center and right plots; Fig. S6). Overall, we find that cTECs are positive for CD205 and CD200 in the human thymus and that the previously published CD49f versus CD200 combination cannot be used to clearly distinguish cTECs from mTECs in the human thymus.

We also noted distinct subclusters of putative Nurse cells (clusters 1, 2, 3) based on the mRNA expression of both cTEC marker genes (PRSS16, PSMB11, LY75) and the pan-leukocyte marker PTPRC derived from its internalized thymocytes (Fig. S7A, B). Differential gene expression analysis suggested that each Nurse cell subcluster contained distinct subsets of leukocytes. Both clusters 1 and 2 contain mainly thymocytes (expressing RAG1, CD3E) (Fig. S7B). Cluster 2 is distinguished from cluster 1 by its high expression of proliferation gene signature (MKI67, TOP2A) (Fig. S7B, C). Cluster 3 showed weak and bimodal cTEC gene signatures relative to clusters 1 and 2, suggesting population heterogeneity within cluster 3. We therefore reclustered cluster 3 with higher resolution to generate 7 subclusters (Fig. S7D). Cluster 0 showed the strongest cTEC gene signature, while clusters 1 through 6 express cTEC signature genes PRSS16 and PSMB11 only weakly. In contrast, they express markers of other classical immune cell types such as dendritic cells, B cells, and macrophages. Expression of thymocyte markers TRAC and RAG1 in cluster 0 indicated that this cluster was a true Nurse cell population. Interestingly, markers of B cells (MS4A1, CD79A, CD79B) and some dendritic cells subsets (SPIB, CLEC4C, IRF4) can also be found in cluster 0, suggesting the presence of a small population of Nurse cells that can engulf other immune cell types.

## Largely consistent staining patterns across digestion conditions do not explain variations across studies

Reliable identification of postnatal TECs and their progenitors, TESCs, will facilitate the understanding of their development, maintenance, and thymic function throughout the lifetime. Recent studies have elevated the importance of this need by demonstrating the critical role of thymus health not just in adaptive immune functions but also in cancer risk, autoimmune disease risk, healthy aging, and longevity.[48–50] While both CD49f and BCAM have both been identified as epithelial stem cell markers in various contexts,[51,52] widespread expression of these markers in TECs (Fig. 5; Fig. S2) suggests that they are not appropriate for identification of rare populations such as TESCs as previously reported.[11] Both our flow cytometry and scRNAseq data are consistent with findings by Haunerdinger et al.[13] that all human TECs express CD49f (ITGA6), with CD200 expression distinguishing a CD49f(hi) population and a CD49f(lo) population (Fig. 5A, left; Fig. 5B, second row). Similarly, a large proportion of TECs express BCAM (Fig. 5A, right; Fig. 5B, third row). These results contrast with the reported low frequency of TECs expressing these two markers.[11]

We hypothesized that the differences in expression and the staining patterns are due to different tissue digestion conditions, as surface markers have varying levels of susceptibility to cleavage by digestive enzymes.[53,54] The common procedure for human thymus tissue processing typically involves the use of a mixture of collagenase, neutral protease, DNase, and occasionally trypsin. Therefore, we compared our digestion protocol with those from published studies to assess how different digestion




C

| Study | Enzyme Mix |
|---|---|
| This study | 0.6 mg/ml Collagenase IV<br>1.6 U/ml Neutral Protease (Dispase) |
| Haunerdinger *et al.* | 0.2 mg/ml Liberase TM |
| Huisman *et al.* | 0.5 mg/ml Collagenase II<br>0.5 mg/ml Collagenase/Dispase |
| Ragazzini *et al.* | 0.4 mg/ml Collagenase D<br>0.6 mg/ml Dispase II |

*same amount of DNase I was added to each condition

**Figure 5** Flow staining pattern of select TEC markers across digestion conditions. (A) Feature plot of expression of ITGA6 and BCAM across human TEC populations. (Left) Highest expression of ITGA6 is seen in the BMC TECs. (Right) BCAM is expressed by a large fraction of BMC TECs and mTECs. (B) Comparison of TEC markers (EpCAM, CD205, CD49f, CD200, BCAM) across 4 digestion enzyme mixes (see panel C). (Top) CD205 staining intensity under different digestion conditions. (Middle) CD49f and CD200 staining intensity under different digestion conditions. (Bottom) BCAM staining intensity under different digestion conditions. (C) Four digestive enzyme mixes used in human TEC studies.

Downloaded from academic.oup.com/jimmunol/article/215/11/vkag281/9045887 by Cold Spring Harbor Laboratory user on 16 November 2026

cocktails[9,11,13] influence TEC surface marker detection by antibodies (Fig. 5C). To minimize unwanted variation and limit our analysis to only changes in the digestion enzyme mix, we first obtained 1.2 g tissue fragments from 4 different areas of a thymus sample, diced them into smaller fragments suitable for digestion, pooled and mixed them, and then divided equally into the 4 different digestion conditions. As the original protocols also varied slightly in the digestion duration (from 20 to 45 min) per round, we further controlled for that factor by fixing the duration to 25 min per round. Therefore, the differences were limited to the type and concentration of the enzyme mixture used. Our results indicate that these 4 digestion conditions produced largely consistent staining patterns, with some differences in signal intensity and proportions depending on the marker. For instance, CD205 expression showed variable frequencies across the 4 digestion conditions, ranging from 5% to 14% of the total TEC population (Fig. 5B, top row). Excessive cleavage of CD205 in some groups may have resulted in reduced staining intensity, which contributed to the reduced cell frequencies. Similarly, while the CD49f versus CD200 staining pattern is largely consistent, we see slight differences in the cell frequencies (Fig. 5B, second row).

These variations can arise due to the difference in type and concentration of the enzyme mixtures used in different studies or the use of different antibody clones. A surface marker can be cleaved by digestive enzymes yet still be able to bind its corresponding antibody if the portion of the protein containing the epitope remains intact on the cell surface. The discrepancy between our BCAM+ TEC percentage and the published results may be due to differences in antibody clones used. Therefore, we compared the BCAM antibody clone used in the original report to the antibody clone we used in our flow panel (Fig. S8). The staining pattern for BCAM using the B64 clone again resembled our previous staining pattern. Furthermore, when plotting the two BCAM antibody clones against each other, the thin diagonal pattern indicated that these two clones were indeed staining for the same target on the cell surface. Our data indicate that most of the mTEC population are BCAM+, whereas only a small subset appeared positive in the original report. Therefore, we conclude that the observed differences in BCAM staining might be due to other factors such as flow cytometry gating strategy and not the antibody clones used.

## Establishing a core flow panel gating strategy for the identification of major TEC subsets

To promote consistency in TEC studies, we established a flow cytometry panel for the identification of major human TEC subsets. We provide our flow cytometer configuration, gating strategy, and corresponding mRNA expression of those markers by scRNAseq (Fig. 6A; Table S2). In our flow cytometry experiments with human TECs, we noticed that cTECs are typically higher on the forward scatter area (FSC-A) and side scatter area (SSC-A) parameters, indicating that they tend to be larger and internally more complex compared with other TEC subsets. We therefore lower the voltage of FSC-A and SSC-A parameters significantly when working with TECs compared with working with smaller cells such as lymphocytes. We first gate on all cells but exclude the debris at the lower left corner. We extend the top and right edges of the gate beyond the visible edge of the plot window (usually $10^5$ on a conventional cytometer) but remove the doublets piled on the maximum edge during the subsequent singlet-gating step. The second gate identifies the EpCAM+ cells using the EpCAM-BV421 antibody and an open detector in the 500 to 650 nm range excited by the 405 nm laser. In our cytometer, detectors used for fluorophores BV510, BV605, or BV650 usually give the best separation between the EpCAM+ cells and the autofluorescent non-TEC population. Gating on EpCAM+ cells first allows for cleaner gating on the quality control gates: singlets and viability gating. This is generally true if the cells of interest make up only a small percentage of the entire sample, because the light scatter characteristics from the major cell population can overwhelm and obscure the boundaries between the positive and negative signals in the smaller population. Subsequent singlet-gating employs the standard parameters FSC height vs FSC width and SSC height vs SSC width. Because cTECs appear larger and more complex than the other TEC subsets, there is more variation in the singlet-gating parameters, so the singlet gate tends to be "thicker" relative to singlet gates for small and uniformly sized cells such as lymphocytes. Dead cells are removed after the singlet-gating. As we had already gated on the EpCAM+ cells in the second gate, the border between the live and dead EpCAM+ cells is much cleaner (Fig. 6A, fifth panel from the left). Thus, one can go up the gating tree and add this live-dead gate as the second gate prior to gating on EpCAM + cells if one wishes. Adding this step can at times help to better distinguish the border between EpCAM+ and EpCAM − cells by removing autofluorescent signals from the dead cell population. Additionally, because the live gate was drawn based on the EpCAM+ cells, there is no risk of accidentally removing any EpCAM+ cells. If this extra step is not taken, then it is advisable to plot the second gate once more to "clean-up" the EpCAM+ gate (Fig. 6A, right-most plot).

We use the following core parameters to identify the major human TEC populations: EpCAM, autofluorescence, viability dye, CD205, CD24, CD104, and HLA-DR. CD24 is a marker previously identified in the most mature mTEC population called mimetic TECs, which closely mimics cell types found in the periphery such as muscle and neurons (Fig. 4A).[11] CD104 expression has been associated with pre–Aire-expressing immature mTECs as well as TEC progenitors in in vitro differentiation studies of human pluripotent stem cells.[9,55] In our dataset, we identified BMC TECs with the highest expression of CD104, followed by mTEC lo. To identify the major TEC subsets, we plot CD205 versus CD24. There are 3 populations visible, CD205 + CD24−, CD205 − CD24+, and CD205 − CD24 − (Fig. 6B). Gating on the CD205+ cells, we can see that cTECs are distributed higher on the FSC-A and SSC-A plot relative to other TECs, as described previously (Fig. 6B, second row). As mTECs mature, their expression level of EpCAM also tends to increase. This is observed for the CD205 − CD24+ mTECs in both the flow data and the scRNAseq data, consistent with the maturity of these cells (Fig. 6B, third row; Fig. 6C, left-most plot). The remaining CD205 − CD24− TECs contain all other subsets, including immature TECs and nonmimetic mTECs across their developmental stages. CD104 and HLA-DR can be used together to assess the developmental stages within this population, where immature

Downloaded from academic.oup.com/jimmunol/article/215/11/vkag281/9045887 by Cold Spring Harbor Laboratory user on 16 November 2026

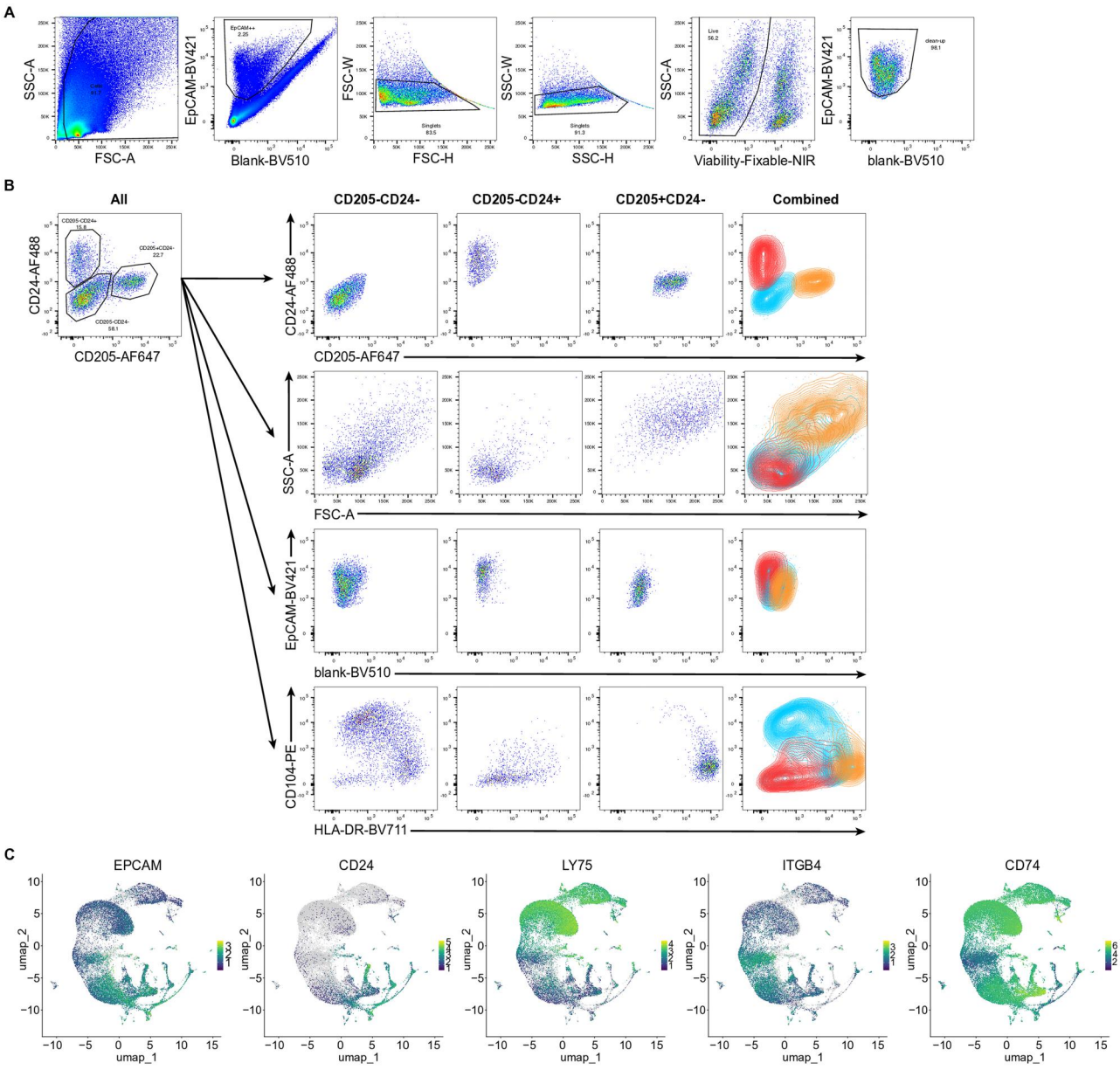



**Figure 6** Core flow panel gating strategy for the identification of major human TEC subsets. (A) Gating tree and quality control gates for the identification of TECs: from left to right, gate on cells and remove debris, gate on EpCAM+ cells, singlet gate, singlet gate, live gate, and clean-up gate to remove residual EpCAM− cells. (B) Characterization of major human TEC populations by CD205, CD24, CD104, and HLA-DR. (Top) TECs can be subsetted by CD205+ CD24− (cTECs), CD205− CD24+ (mimetic TECs), and CD205− CD24− (a mixture of all other TECs, including immature TECs and mTECs at various developmental stages). (Top middle) Distribution of these 3 TEC subsets on the FSC-A versus SSC-A plot. (Bottom middle) Relative distribution of these 3 TEC subsets by level of EpCAM expression and autofluorescence (blank BV510 channel). (Bottom) Characterization of these 3 TEC subsets by maturation markers HLA-DR and CD104. (C) UMAP plot of the same markers used in the flow panel, showing concordance in protein and RNA expression pattern of these markers across the TEC subsets. FSC-H, forward scatter height; FSC-W, forward scatter width; SSC-H, side scatter height; SSC-W, side scatter width.

TECs are CD104 + HLA-DR(lo)/− (Fig. 6B, fourth row). As development progresses, mTECs will first increase and then decrease their expression of HLA-DR, with a concomitant decrease in CD104 expression. Plotting CD104 and HLA-DR within the CD24+ TECs, we see that they are mostly double negative for these markers, further supporting the maturity of these cells (Fig. 6B, fourth row, second column). Similar relative expression of these markers can be seen across the cell types in the scRNAseq data, adding confidence to the validity of these results (Fig. 6C). Note that CD74 UMAP plot is presented here instead of HLA-DR because the 10x Genomics Flex scRNAseq method is probe based and thus excludes HLA genes due to high degrees of polymorphism (Fig. 6C, right-most plot). However, CD74 is critical in the major histocompatibility complex class II peptide presentation pathway and correlates with HLA-DR expression in various contexts.[56–58] One can see that both CD74, a proxy for HLA-DR, and

Downloaded from academic.oup.com/jimmunol/article/215/11/vkag281/9045887 by Cold Spring Harbor Laboratory user on 16 November 2026

ITGB4, which codes for CD104, agree well with the flow cytometry data in terms of relative expression among the TEC subsets. Together, these surface markers can be used to assess and FACS sort the major subsets of the human TEC population.

# Discussion

Investigating human TEC biology typically involves a long process of dissection, thymocyte release, digestion, enrichment, and FACS sorting to isolate a pure TEC population for downstream assays. Irreproducible and contradictory findings on TEC biology can be a combination of biological and technical variations in these processing steps. We investigated those through a series of experiments including tissue size and the comparison of differences in the digestion enzymes and the antibodies used. We standardized the tissue processing protocol and established a 7-parameter flow cytometric gating strategy to consistently identify the major human TEC subsets.

Reproducibility starts with a representative sample of the organ. We assessed this by taking the same amount of tissue from different regions of a human thymus sample. Using the proportion of cTECs to mTECs as a proxy for tissue representativeness, our data suggest that 1 g of tissue, while it may not be the minimum size, is sufficient to provide a representative sample of the neonatal human thymus tissue. As the thymus undergoes dramatic morphological changes across the lifespan,[59–61] the minimum tissue size to obtain a representative sample is likely to change with age and should be assessed in future studies.

In addition to sampling and biological variations, differences in each step of the tissue processing protocol from digestion and enrichment to data acquisition and gating strategy can alter the final interpretation of the data. For example, while the reliability of CD205 as a cTEC marker has come into question,[13] we confirmed using flow cytometry, dot blot, and scRNAseq that it is a reliable marker to identify the human cTEC population. We hypothesized that qualitative differences such as the nature of the tissue digestion enzyme cocktail and the flow cytometric analysis strategies are largely responsible for the observed variations in marker expression. Indeed, when comparing digestion enzyme cocktails, we saw differential staining intensity of CD205, indicating some enzyme cocktails are more likely to cleave CD205. Additionally, we saw that CD205+ TECs were situated much higher in the FSC-A versus SSC-A plot. If the voltage setting on the cytometer is high enough during sample acquisition, cTECs will pile up against the edge of the flow plot. Standard flow cytometric gating strategy will remove these cells from downstream analysis. Differences in marker expression of CD49f and BCAM we observed are likely to be explained by similar technical differences.

Intercellular protein transfer might also be a contributing factor as both TECs and thymocytes transfer proteins to other thymic cell types.[27–32,35,38,62] Our analysis of CD45 and CD200 expression in TECs, particularly cTECs, may be explained by this mechanism. Among the TEC subsets, cTECs exhibit a uniquely close interaction with thymocytes with so-called nurse cells internalizing as many as 200 thymocytes simultaneously.[63,64] This close contact between cTECs and thymocytes may increase the probability of intercellular protein transfer and influence the identification and sorting of cell types by protein expression. This has important implications for antibody-based cell enrichment protocols. In the case of TECs, the use of pan-immune cell markers to deplete immune cells may inadvertently deplete other cells that have acquired the protein. The effect can be magnified when combined with magnetic field-based depletion approaches. In contrast, the traditional panning approach we follow here may prove advantageous due to the preferential binding of the intended target cells that express high levels of the antibody targets, effectively shielding other cells from binding to the panning plate surface. How much effect this has on unintentional depletion of nurse cells requires further investigation.

The large population of nurse cells (>5,000 cells) in our dataset allowed deeper characterization, revealing putative nurse subsets that contain distinct leukocyte populations. Engulfment of thymocytes and macrophages has been described in animal models.[65] Our data suggested that human nurse cells may also engulf B cells and various myeloid immune cells. Future studies on human thymic nurse cells should focus on resolving immediate technical challenges associated with nurse cell identification: (i) assess unintentional depletion of thymic nurse cells by antibody and magnet-based enrichment methods and (ii) verify doublet/multiplet quality control steps in both flow cytometric and computational approaches because nurse cells are naturally occurring cell multiplets and not technical multiplets. Because of this limitation, we cannot say for certain whether cluster 13 contains proliferating nurse cells or proliferating thymocytes or both. Our study examined 3 thymi by RNA sequencing, spanning an age range from 3 mo to 4 yr from both male and female donors. Despite this range, the CD205pos and CD205neg dataset, which were sorted from the same sample (HT67), partitions cleanly with the cTEC and mTEC subsets of the other samples even without additional scRNAseq integration procedure. Future work examining age and sex effects in a larger cohort will further our understanding of these biological factors.

To summarize, these factors at each step of the initial tissue processing can influence the final analysis of TEC biology, such as cell type identification and quantification. Here, we provided recommendations for the processing of human thymus samples to identify and isolate TEC subsets. In our analysis of 4 digestion conditions, we find that the protocol using Collagenase D and Dispase II[11] appeared to best preserve cell marker epitopes for the markers we assessed. At the flow cytometry step, the voltages for FSC-A and SSC-A detectors should be lowered such that the cTEC population is within view. As every cytometer is different, it is advisable to gate on the CD205+ cTEC population first, then perform backgating onto the FSC-A versus SSC-A plot to see where the cTECs lie and adjust the voltages accordingly. Following the FSC-A and SSC-A gate, EpCAM and autofluorescence should be used first to identify the TECs as this “cleans up” the TEC population borders for the subsequent singlet and viability gates. Following these gates, one may wish to replot the EpCAM versus autofluorescence plot to view the EpCAM+ cell population border more clearly and gate out any residual contaminating cells. Finally, the use of CD24, CD205, CD104, and HLA-DR can be used to identify the major TEC subsets. We hope that these recommendations will improve the reproducibility in research of TEC biology and accelerate the development of therapeutics aimed at improving thymic and immunological health.

Downloaded from academic.oup.com/jimmunol/article/215/11/vkag281/9045887 by Cold Spring Harbor Laboratory user on 16 November 2026

## Acknowledgments

This work was performed with assistance from Cold Spring Harbor Laboratory Shared Resources, including Flow Cytometry, Next Generation Sequencing and Single Cell Shared Resources, which are supported by the Cancer Center Support Grant 5P30CA045508.

## Author contributions

Yong Lin (Conceptualization [Equal], Data curation [Lead], Formal analysis [Lead], Investigation [Lead], Visualization [Lead], Writing—original draft [Equal]), Madison E. Lapine (Investigation [Supporting], Writing—review & editing [Supporting]), Deena M. Netz (Investigation [Supporting], Writing—review & editing [Supporting]), Sarah R Chapin (Investigation [Supporting], Writing—review & editing [Supporting]), Rishvanth K Prabakar (Investigation [Supporting], Writing—review & editing [Supporting]), and Meyer V. Hannah (Conceptualization [Equal], Funding acquisition [Lead], Project administration [Lead], Supervision [Lead], Writing—original draft [Equal])

## Supplementary material

Supplementary material is available at *The Journal of Immunology Online*.

## Funding

The research was supported by the Simons Center for Quantitative Biology at Cold Spring Harbor Laboratory, the Cold Spring Harbor Laboratory and Northwell Health Affiliation, the Rita Allen Foundation, and National Institutes of Health grants S10OD028632-01 and 1R01AI167862.

## Conflicts of interest

None declared.

## Data availability

The 10x Genomics Flex scRNAseq FASTQ files and processed data objects (seurat, anndata) as well as additional metadata are accessible from dbGAP (access controlled for Health/Medical/Biomedical Use per Institutional Review Board): phs004985.v1. Data to reproduce figures are provided in the github repository. The complete human thymus tissue processing protocol is available at https://dx.doi.org/10.17504/protocols.io.x54v99781v3e/v1 Any additional data are available upon request. All data analyses were conducted with R $\geq$ 4.6.0 and python $\geq$ 3.11. Code for all data analyses and manuscript figures are at https://github.com/meyer-lab-cshl/isolation_and_characterization_of_htecs (version JI-accepted at: 10.5281/zenodo.23020449).

## References

1. Hirakawa M et al. Fundamental parameters of the developing thymic epithelium in the mouse. Sci Rep. 2018;8:11095. https://doi.org/10.1038/s41598-018-29460-0
2. Sakata M, Ohigashi I, Takahama Y. Cellularity of thymic epithelial cells in the postnatal mouse. J Immunol. 2018;200:1382–1388. https://doi.org/10.4049/jimmunol.1701235
3. Moses A et al. Comprehensive phenotypic analysis of diverse FOXN1 variants. J Allergy Clin Immunol. 2023;152:1273–1291.e15. https://doi.org/10.1016/j.jaci.2023.06.019
4. Du Q et al. FOXN1 compound heterozygous mutations cause selective thymic hypoplasia in humans. J Clin Invest. 2019;129:4724–4738. https://doi.org/10.1172/JCI127565
5. Aytekin ES, Cagdas D. APECED and the place of AIRE in the puzzle of the immune network associated with autoimmunity. Scand J Immunol. 2023;98:e13299. https://doi.org/10.1111/sji.13299
6. Campinoti S et al. Reconstitution of a functional human thymus by postnatal stromal progenitor cells and natural whole-organ scaffolds. Nat Commun. 2020;11:6372. https://doi.org/10.1038/s41467-020-20082-7
7. Bautista JL et al. Single-cell transcriptional profiling of human thymic stroma uncovers novel cellular heterogeneity in the thymic medulla. Nat Commun. 2021;12:1096. https://doi.org/10.1038/s41467-021-21346-6
8. Michelson DA, Hase K, Kaisho T, Benoist C, Mathis D. Thymic epithelial cells co-opt lineage-defining transcription factors to eliminate autoreactive T cells. Cell. 2022;185:2542–2558.e18. https://doi.org/10.1016/j.cell.2022.05.018
9. Huisman BD et al. Cross-species analyses of thymic mimetic cells reveal evolutionarily ancient origins and both conserved and species-specific elements. Immunity. 2025;58:108–123.e7. https://doi.org/10.1016/j.immuni.2024.11.025
10. Yayon N et al. A spatial human thymus cell atlas mapped to a continuous tissue axis. Nature. 2024;635:708–718. https://doi.org/10.1038/s41586-024-07944-6
11. Ragazzini R et al. Defining the identity and the niches of epithelial stem cells with highly pleiotropic multilineage potency in the human thymus. Dev Cell. 2023;58:2428–2446.e9. https://doi.org/10.1016/j.devcel.2023.08.017
12. Hjorthaug HS, Heimli M, Flåm ST, Lie BA. Multimodal single-cell profiling identifies nclTECs and links chromatin remodeling to TEC differentiation and self-antigen expression modes. iScience. 2026;29:116916. https://doi.org/10.1016/j.isci.2026.116916
13. Haunerdinger V et al. Novel combination of surface markers for the reliable and comprehensive identification of human thymic epithelial cells by flow cytometry: quantitation and transcriptional characterization of thymic stroma in a pediatric cohort. Front Immunol. 2021;12:740047. https://doi.org/10.3389/fimmu.2021.740047
14. Dragin N et al. Estrogen-mediated downregulation of AIRE influences sexual dimorphism in autoimmune diseases. J Clin Invest. 2016;126:1525–1537. https://doi.org/10.1172/JCI81894
15. Yang M-T, Li J, Matsuda-Lennikov M, Crossman A, Takahama Y. Preparation of single-cell suspension of mouse thymic epithelial cells and staining of intracellular molecules for flow

Downloaded from academic.oup.com/jimmunol/article/215/11/vkag281/9045887 by Cold Spring Harbor Laboratory user on 16 November 2026

cytometric analysis. J Vis Exp. 2024;209:e66945. https://doi.org/10.3791/66945
16. Koch F, Kämpgen E, Schuler G, Romani N. Effective enrichment of murine epidermal langerhans cells by a modified (mismatched) panning technique. J Invest Dermatol. 1992;99:803–807. https://doi.org/10.1111/1523-1747.ep12614764
17. Wysocki LJ, Sato VL. "Panning" for lymphocytes: a method for cell selection. Proc Natl Acad Sci U S A. 1978;75:2844–2848. https://doi.org/10.1073/pnas.75.6.2844
18. Hao Y et al. Dictionary learning for integrative, multimodal and scalable single-cell analysis. Nat Biotechnol. 2024;42:293–304. https://doi.org/10.1038/s41587-023-01767-y
19. Wolf FA, Angerer P, Theis FJ. SCANPY: large-scale single-cell gene expression data analysis. Genome Biol. 2018;19:15. https://doi.org/10.1186/s13059-017-1382-0
20. Lopez R, Regier J, Cole MB, Jordan MI, Yosef N. Deep generative modeling for single-cell transcriptomics. Nat Methods. 2018;15:1053–1058. https://doi.org/10.1038/s41592-018-0229-2
21. Gayoso A et al. A Python library for probabilistic analysis of single-cell omics data. Nat Biotechnol. 2022;40:163–166. https://doi.org/10.1038/s41587-021-01206-w
22. Xu C et al. Probabilistic harmonization and annotation of single-cell transcriptomics data with deep generative models. Mol Syst Biol. 2021;17:e9620. https://doi.org/10.15252/msb.20209620
23. Wang X, Park J, Susztak K, Zhang NR, Li M. Bulk tissue cell type deconvolution with multi-subject single-cell expression reference. Nat Commun. 2019;10:380. https://doi.org/10.1038/s41467-018-08023-x
24. Dobin A et al. STAR: ultrafast universal RNA-seq aligner. Bioinformatics. 2013;29:15–21. https://doi.org/10.1093/bioinformatics/bts635
25. Xing Y, Hogquist KA. Isolation, identification, and purification of murine thymic epithelial cells. J Vis Exp. 2014;90:e51780.
26. Stoeckle C et al. Isolation of myeloid dendritic cells and epithelial cells from human thymus. J Vis Exp. 2013;70:e50951.
27. Wang H-X, Qiu Y-R, Zhong X-P. Intercellular protein transfer from thymocytes to thymic epithelial cells. PLoS One. 2016;11:e0152641. https://doi.org/10.1371/journal.pone.0152641
28. Gallegos AM, Bevan MJ. Central tolerance to tissue-specific antigens mediated by direct and indirect antigen presentation. J Exp Med. 2004;200:1039–1049. https://doi.org/10.1084/jem.20041457
29. Aschenbrenner K et al. Selection of Foxp3+ regulatory T cells specific for self antigen expressed and presented by Aire + medullary thymic epithelial cells. Nat Immunol. 2007;8:351–358. https://doi.org/10.1038/ni1444
30. Koble C, Kyewski B. The thymic medulla: a unique microenvironment for intercellular self-antigen transfer. J Exp Med. 2009;206:1505–1513. https://doi.org/10.1084/jem.20082449
31. Hubert F-X et al. Aire regulates the transfer of antigen from mTECs to dendritic cells for induction of thymic tolerance. Blood. 2011;118:2462–2472. https://doi.org/10.1182/blood-2010-06-286393
32. Lei Y et al. Aire-dependent production of XCL1 mediates medullary accumulation of thymic dendritic cells and contributes to regulatory T cell development. J Exp Med. 2011;208:383–394. https://doi.org/10.1084/jem.20102327
33. Taniguchi RT et al. Detection of an autoreactive T-cell population within the polyclonal repertoire that undergoes distinct autoimmune regulator (Aire)-mediated selection. Proc Natl Acad Sci U S A. 2012;109:7847–7852. https://doi.org/10.1073/pnas.1120607109
34. Perry JSA et al. Distinct contributions of Aire and antigen-presenting-cell subsets to the generation of self-tolerance in the thymus. Immunity. 2014;41:414–426. https://doi.org/10.1016/j.immuni.2014.08.007
35. Leventhal DS et al. Dendritic cells coordinate the development and homeostasis of organ-specific regulatory T cells. Immunity. 2016;44:847–859. https://doi.org/10.1016/j.immuni.2016.01.025
36. Kroger CJ, Spidale NA, Wang B, Tisch R. Thymic dendritic cell subsets display distinct efficiencies and mechanisms of intercellular MHC transfer. J Immunol. 2017;198:249–256. https://doi.org/10.4049/jimmunol.1601516
37. Perry JSA et al. Transfer of cell-surface antigens by scavenger receptor CD36 promotes thymic regulatory T cell receptor repertoire development and allo-tolerance. Immunity. 2018;48:923–936.e4. https://doi.org/10.1016/j.immuni.2018.04.007
38. Vobořil M et al. A model of preferential pairing between epithelial and dendritic cells in thymic antigen transfer. eLife. 2022;11:e71578. https://doi.org/10.7554/eLife.71578
39. Rouse RV, Bolin LM, Bender JR, Kyewski BA. Monoclonal antibodies reactive with subsets of mouse and human thymic epithelial cells. J Histochem Cytochem. 1988;36:1511–1517. https://doi.org/10.1177/36.12.2461413
40. de Maagd RA et al. The human thymus microenvironment: heterogeneity detected by monoclonal anti-epithelial cell antibodies. Immunology. 1985;54:745–754.
41. McKay PF et al. The gp200-MR6 molecule which is functionally associated with the IL-4 receptor modulates B cell phenotype and is a novel member of the human macrophage mannose receptor family. Eur J Immunol. 1998;28:4071–4083. https://doi.org/10.1002/(SICI)1521-4141(199812)28:12<4071::AID-IMMU4071>3.0.CO; 202-O
42. Palmer DB, Crompton T, Marandi MB, George AJ, Ritter MA. Intrathymic function of the human cortical epithelial cell surface antigen gp200-MR6: single-chain antibodies to evolutionarily conserved determinants disrupt mouse thymus development. Immunology. 1999;96:236–245. https://doi.org/10.1046/j.1365-2567.1999.00691.x
43. Forrester MA et al. Similarities and differences in surface receptor expression by THP-1 monocytes and differentiated macrophages polarized using seven different conditioning regimens. Cell Immunol. 2018;332:58–76. https://doi.org/10.1016/j.cellimm.2018.07.008
44. Sun S et al. CD90 marks a Mesenchymal program in human thymic epithelial cells in vitro and in vivo. Front Immunol. 2022;13:846281. https://doi.org/10.3389/fimmu.2022.846281
45. Li A, Liu X, Duan B, Ma J. Thymic nurse cells support CD4-CD8+ thymocytes to differentiate into CD4 + CD8+ cells. Cell Mol Immunol. 2005;2:301–305.
46. Hendrix TM et al. Thymic nurse cells exhibit epithelial progenitor phenotype and create unique extra-cytoplasmic

Downloaded from academic.oup.com/jimmunol/article/215/11/vkag281/9045887 by Cold Spring Harbor Laboratory user on 16 November 2026

membrane space for thymocyte selection. Cell Immunol. 2010; 261:81–92. https://doi.org/10.1016/j.cellimm.2009.11.004
47. Nakagawa Y et al. Thymic nurse cells provide microenvironment for secondary T cell receptor α rearrangement in cortical thymocytes. Proc Natl Acad Sci U S A. 2012;109: 20572–20577. https://doi.org/10.1073/pnas.1213069109
48. Bernatz S et al. Thymic health consequences in adults. Nature. 2026;652:986–994. https://doi.org/10.1038/s41586-026-10242-y
49. Bernatz S et al. Thymic health and immunotherapy outcomes in patients with cancer. Nature. 2026;652:995–1003. https://doi.org/10.1038/s41586-026-10243-x
50. Kooshesh KA, Foy BH, Sykes DB, Gustafsson K, Scadden DT. Health consequences of thymus removal in adults. N Engl J Med. 2023;389:406–417. https://doi.org/10.1056/NEJMoa2302892
51. Krebsbach PH, Villa-Diaz LG. The role of integrin α6 (CD49f) in stem cells: more than a conserved biomarker. Stem Cells Dev. 2017;26:1090–1099. https://doi.org/10.1089/scd.2016.0319
52. Sasamoto Y et al. Limbal BCAM expression identifies a proliferative progenitor population capable of holoclone formation and corneal differentiation. Cell Rep. 2022;40:111166. https://doi.org/10.1016/j.celrep.2022.111166
53. Autengruber A, Gereke M, Hansen G, Hennig C, Bruder D. Impact of enzymatic tissue disintegration on the level of surface molecule expression and immune cell function. Eur J Microbiol Immunol (Bp). 2012;2:112–120. https://doi.org/10.1556/EuJMI.2.2012.2.3
54. Bondonese A et al. Impact of enzymatic digestion on single cell suspension yield from peripheral human lung tissue. Cytometry A. 2023;103:777–785. https://doi.org/10.1002/cyto.a.24777
55. Soh C-L et al. FOXN1GFP/w reporter hESCs enable identification of Integrin-β4, HLA-DR, and EpCAM as markers of human PSC-derived FOXN1+ thymic epithelial progenitors. Stem Cell Rep. 2014;2:925–937. https://doi.org/10.1016/j.stemcr.2014.04.009
56. Romagnoli P, Germain RN. The CLIP region of invariant chain plays a critical role in regulating major histocompatibility complex class II folding, transport, and peptide occupancy. J Exp Med. 1994;180:1107–1113. https://doi.org/10.1084/jem.180.3.1107
57. Badve S, Deshpande C, Hua Z, Lennart L. Expression of invariant chain (CD 74) and major histocompatibility complex (MHC) class II antigens in the human fetus. J Histochem Cytochem. 2002;50:473–482. https://doi.org/10.1177/002215540205000404
58. Datta MW, Shahsafaei A, Nadler LM, Freeman GJ, Dorfman DM. Expression of MHC class II-associated invariant chain (Ii; CD74) in thymic epithelial neoplasms. Appl Immunohistochem Mol Morphol. 2000;8:210–215. https://doi.org/10.1097/00129039-200009000-00007
59. Simpson JG, Gray ES, Beck JS. Age involution in the normal human adult thymus. Clin Exp Immunol. 1975;19:261–265.
60. Singh J, Singh AK. Age-related changes in human thymus. Clin Exp Immunol. 1979;37:507–511.
61. Flores KG, Li J, Sempowski GD, Haynes BF, Hale LP. Analysis of the human thymic perivascular space during aging. J Clin Invest. 1999;104:1031–1039. https://doi.org/10.1172/JCI7558
62. Millet V, Naquet P, Guinamard RR. Intercellular MHC transfer between thymic epithelial and dendritic cells. Eur J Immunol. 2008;38:1257–1263. https://doi.org/10.1002/eji.200737982
63. de Waal Malefijt R, Leene W, Roholl PJ, Wormmeester J, Hoeben KA. T cell differentiation within thymic nurse cells. Lab Invest. 1986;55:25–34.
64. Li Y, Pezzano M, Philp D, Reid V, Guyden J. Thymic nurse cells exclusively bind and internalize CD4 + CD8+ thymocytes. Cell Immunol. 1992;140:495–506. https://doi.org/10.1016/0008-8749(92)90214-a
65. Samms M, Martinez M, Fousse S, Pezzano M, Guyden JC. Circulating macrophages as well as developing thymocytes are enclosed within thymic nurse cells. Cell Immunol. 2001; 212:16–23. https://doi.org/10.1006/cimm.2001.1836

Downloaded from academic.oup.com/jimmunol/article/215/11/vkag281/9045887 by Cold Spring Harbor Laboratory user on 16 November 2026

© The Author(s) 2026. Published by Oxford University Press on behalf of The American Association of Immunologists.
This is an Open Access article distributed under the terms of the Creative Commons Attribution-NonCommercial License (https://creativecommons.org/licenses/by-nc/4.0/), which permits non-commercial re-use, distribution, and reproduction in any medium, provided the original work is properly cited. For commercial re-use, please contact reprints@oup.com for reprints and translation rights for reprints. All other permissions can be obtained through our RightsLink service via the Permissions link on the article page on our site—for further information please contact journals.permissions@oup.com.
The Journal of Immunology, 2026, 215, 1–14
https://doi.org/10.1093/jimmun/vkag281
Research Article